PERFORMANCE EVALUATION OF SILICON-BASED PHOTOVOLTAIC MODULES FOUND IN THE KENYAN MARKET

NJERU ELOSY GATAKAA

I56/CE/22378/2010

A thesis submitted in partial fulfillment of the requirements for the award of the degree of master of physics **(Electronics and Instrumentation)** in the School of Pure and Applied Sciences of Kenyatta University.

DECLARATION

This thesis is my original work and has not been presented for a degree in any other university

Njeru Elosy Gatakaa

Department of Physics

Kenyatta University.

Signature…….. Date……

This thesis has been submitted with our approval as university supervisors.

Dr. Mathew K. Munji

Department of Physics

Kenyatta University.

Signature…… Date……

Dr. Walter Njoroge

Department of Physics

Kenyatta University.

Signature…… Date…….

DEDICATION

To my husband Jafford and our daughter Imelda for their unconditional love, support and sacrifice. May Almighty God bless you greatly.

ACKNOWLEDGEMENTS

I wish to express my sincere gratitude to my supervisors Dr. Mathew Munji and Dr. Walter Njoroge of Department of Physics, Kenyatta University for their unreserved guidance during research. Acknowledgements are also made to the University technical staff for their immense support over the entire period of study. I wish to acknowledge my employer the T.S.C for giving me a short term leave for data collection.

Finally I greatly appreciate the moral and material support received from a number of people. I sincerely thank my dear husband Jafford Njeru and my daughter Imeldah Gatugi for their understanding, support and encouragement throughout the period of study. I also express my sincere appreciation to my sister in-law Dorothy Kambura for the great sacrifice. Above all, I thank the Almighty God for giving me the strength and knowledge to achieve this goal.

TABLE OF CONTENTS

LIST OF FIGURES

LIST OF TABLES

ABBREVIATIONS, SYMBOLS AND ACRONYMS

A	Diode ideality factor
a-Si	Amorphous silicon
A_c	Area of the device
b	Temperature coefficient
CdTe	Cadium telluride
CIGS	Copper-Indium- gallium- diselenide
CPV	Concentrating PV
E	Mean measured solar radiation
E_g	Band gap energy
FF	Fill Factor
G	Measured irradiance
I_d	Diode current
I_m	Measured current
I_{max}	Current at maximum power point
I_{mp}	Current at P_{max}
I_n	Normalized current
I_o	Saturation current of the diode
I_{ph}	Photocurrent
I_{sc}	Short circuit current
I_{sh}	Shunt current

K_B	Boltzmann constant (1.38×10^{-23} Joules/ Kelvin)
Mono-c-Si	Mono-crystalline silicon
NOCT	Nominal Operating Cell Temperature
PECVD	Plasma enhanced chemical vapour deposition
P_{in}	Solar power input
P_{max}	Maximum power
P_{out}	Electrical Power output
Poly-c-Si	Poly-crystalline silicon
P_T	Theoretical Power
PV	Photovoltaic
q	Electron charge (1.60×10^{-19} Coulombs)
R_s	Series resistance
R_{sh}	Shunt resistance
SHS_s	Solar home systems
SOC	Standard Test Operating Condition
STC	Standard Test Conditions
SWE	Stablear-Wronski effect
T_a	Ambient temperature
UV	Ultraviolet
V_d	Voltage across the diode
V_m	Measured voltage

V_{mp}	Voltage at P_{max}
V_n	Normalized voltage
V_{oc}	Open circuit voltage
η	Efficiency
φ	Latitude of a location
α	Open circuit Voltage (Voc) temperature coefficient
ϕ	Optimum angle of tilt
β	Short circuit Current (Isc) temperature coefficient

ABSTRACT

Various kinds of photovoltaic (PV) modules have been developed and practically deployed as PV systems over time. The performance of PV modules found in the Kenyan market has not been documented and therefore their reliability and stability in providing an alternative source of energy has not been sufficiently established. In this study the I-V data of Silicon-based mono crystalline, poly crystalline and amorphous modules was collected. The choice of the modules was done randomly depending on their availability, the cost of the modules and their power rating. They were selected randomly from PV module vendors within Nairobi Central Business District (CBD). The manufacturers' specifications were taken. The modules were then mounted at an optimum fixed tilt angle of 15 degrees. Initial measurements of short circuit current I_{sc}, open circuit voltage V_{oc}, ambient temperature and module temperature were taken immediately on mounting the modules. Measurements of current and voltage to obtain I-V data was done daily at solar noon for four months. The back of the module temperature and ambient temperature at the time of measurement was measured using thermocouple while the irradiance at the time of measurement was measured using a pyranometer. The pyranometer was mounted at the plane of array of 15 degrees as the modules. The collected I-V data was normalized and I-V curves were plotted. Performance parameters of the modules were then calculated from the I-V curve. There was a decrease in V_{oc} of the modules with time with the amorphous modules clearly showing the Staebler-Wronski effect. The I_{sc} of the modules showed little variation while P_{max} of the modules had reduced significantly. The P_{max} of most of the modules was found not to match with the manufacturers specifications provided in their data sheet. On inspection of the modules, the 10W polycrystalline module revealed a defect which was as a result of overheating of the cells that contributed greatly to its poor performance in comparison to the other polycrystalline modules. The efficiency of the amorphous modules ranged between 3%- 5% while that of mono crystalline and polycrystalline was above 10%.

CHAPTER ONE

INTRODUCTION

1.1 Background to the Study

The ever increasing world energy demand, the fast depletion of fossil fuels and the unpredictable weather pattern due to global warming have prompted the world to look for alternative source of energy.

In Kenya the weather patterns are friendly in that most of the days have clear sky conditions and at least eight hours of sunshine. Infrastructure investment on hydroelectric power which is the main source of power is low. There are many places that are not served with the national grid and yet they require some source of power. Photovoltaic electrical energy is the most favored source of electrical energy since it is environmentally friendly, readily available and abundant.

New manufacturers have come up and new technologies have emerged to meet the high energy demand by consumers. While more manufacturers and new technologies are emerging, the reliability of solar PV modules becomes a critical performance measure for the success of the industry (Rong *et al*., 2011).

The performance of PV modules has been observed to gradually decrease with operation time (Dunlop and Halton, 2006). Long term performance of PV modules is vital if they have to pay back to the consumer. It is important to investigate the performance parameters of the modules. In order to have maximum sunlight conversion, the tilt and orientation of the modules should be maximized (Akachuku, 2011). According to Duke *et al*. (2010), Kenya has an active market for

photovoltaic (PV) solar home systems (SHSs), with cumulative sales in excess of 100 000 units and current sales of approximately 20 000 modules per year. Small 10-14W single junction amorphous silicon (a-Si) modules dominate the market, largely due to their lower retail price relative to similar sizes of crystalline PV modules. Amorphous silicon modules sell for approximately US$ 5.00 per rated peak watt (Wp) in Kenya while most brands of similarly sized crystalline modules sell for US$ 9.00 per rated Wp.

Despite this commercial success, there is substantial concern about the performance of single junction thin-film a-Si because of the technologies uneven quality record and the uncertainty introduced by short term degradation which occurs when this type of module is initially exposed.

In this study, current-voltage (I-V) data was measured using an I-V curve tracer. The I-V data obtained was used to plot solar cell I-V curves. Solar cell parameters modeled using the one-diode solar cell model, were then extracted from the I-V curves. Solar cell device and performance parameters were extracted and calculated from the I-V modeled curves. Parameters such as short circuit current (I_{sc}), open circuit voltage (V_{oc}), Fill Factor (FF) and current and voltage at maximum power point of the modules (I_{max}, V_{max}) were then calculated. The study analyzed silicon based solar cell technologies commonly found in the Kenyan market. The finding was used to investigate the degradation rates of the modules there by determining the stability and their reliability.

1.2 Statement of the Research Problem

The performance of PV modules once in use differs significantly with time from the specifications provided by the manufacturers. This performance degradation of the modules greatly affects the output of the modules as well as disappointing the user. Kenya has an active

market for photovoltaic (PV) solar home systems (SHSs) with sales of 20 000 modules per year (Duke *et al.,* 2010). The rural consumers are ill-equipped to compare the relative performance of different module types available in the market while others have no idea of different types and therefore go for the cheap retail price. Little research has been done on the performance of the modules available in the Kenyan market. This research aimed at evaluating the performance of modules from three silicon based technologies i.e. three Silicon-based polycrystalline, three Silicon-based mono crystalline and three Silicon-based amorphous which are commonly found in the Kenyan market. This study measured and monitored the I-V data of nine modules selected randomly from three different manufacturers. Their performance parameters were compared to determine their stability under the Kenyan climate as well as compare these parameters with the manufacturer's specifications.

1.3 Objectives of the Research

1.3.1 General Objective

The general objective was to investigate the performance of Silicon-based Photovoltaic modules from different manufacturers found in the Kenyan market.

1.3.2 Specific Objectives

The specific objectives were:

i. To measure the short circuit current (I_{sc}) and open circuit voltage (V_{oc}) of the modules every day at solar noon for four months.
ii. To measure and collect the current-voltage data, back of the module temperature, ambient temperature and solar irradiance every day at solar noon for four months.

iii. To model the I-V data using the one diode model and plotting the I-V curves.

iv. To extract the performance parameters of each module i.e. I_{sc}, V_{oc}, the Fill Factor (FF), Efficiency (η) and current (I_{max}) and voltage (V_{max}) at maximum power Point (P_{max}) from the I-V curves.

v. To carry out daily visual inspection of the modules to check for any observable changes such as damaged cells or the layer of dust cover on the modules.

1.4 Rationale of the Study

There are several types of photovoltaic (PV) modules from different manufacturers available in the Kenyan market. The specifications provided in the manufacturers' data sheet indicate high performance and high reliability. These specifications are always measured at Standard Test Conditions (STC: module temperature = 25^{o} C, Irradiance = $1000 W/m^2$ and Air mass = 1.5) that is not very representative of the real conditions in which the PV devices have to operate.

Research has shown that the output of PV modules differs significantly once exposed to outdoor conditions (Ryan *et al*., 2012) thus their reliability and stability in providing alternative source of energy being questionable. This research investigated the performance of nine PV modules from three different technologies from different manufacturers, which are commonly available in the Kenyan market. The parameters investigated include: short circuit current, the open circuit voltage, the Fill Factor and the efficiency of the modules by measuring solar irradiance, back of the module temperature, and how the ambient temperature conditions affect the output of the modules as well as how these factors cause deterioration of the PV modules.

1.5 Location of Area of Study

The research was carried out in Chuka, North East of Nairobi on a location whose latitude is 0.33º South and longitude 37.65º East. The data was collected in the months of August to November. The weather pattern of the location is: From mid-December to mid-March it is hot and dry, mid-March to July long rains, August to mid-October it is cooler dry season, and from mid-October to mid-December is short rains. The temperatures are moderate fluctuating between the highs of 29 degrees and lows of 16 degrees Celsius in January and highs of 24 degrees and lows of 7 degrees Celsius in July (http://www.Kenya-information-guide.com/Kenya-weather.html).The long rains are expected between the months of March and June while the short rains are expected in October and November.

1.6 Thesis Outline/Organization

The study compares the performance of individual photovoltaic modules under outdoor operation for four months. The nine modules represent three different technologies. The technologies investigated are mono crystalline (c-Si), poly-crystalline (p-Si) and the amorphous silicon (a-Si). These modules represent widely used technologies by the module consumers in Kenya (Duke *et al*., 2010).

Chapter one gives the background to the study, the statement of the research problem, the general objective as well as the specific objectives. It also provides the geographical location of the area of study as well as the weather patterns in the area of study.

Chapter two provides the necessary background and context to the work described in this thesis. Previous studies showing the differences in performance of a variety of technologies are discussed.

Chapter three gives an overview of the various solar cell technologies that exist in the market, photovoltaic performance parameters and provides information on how temperature affects the module performance. It also provides the failure modes of PV modules as well as how the maximum angle of tilt was calculated.

Chapter four provides information the materials and methods that were employed in the collection and analysis of data.

Chapter five gives the results obtained and a discussion of the research findings.

Chapter six provides conclusions and recommendations for further work.

CHAPTER TWO

LITERATURE REVIEW

2.1 Background Information

With rapid economic growth and improvement in living standards, there has been a marked increase in energy consumption in many third world countries. Most countries use fossil fuel, hydroelectric power and nuclear power as a source of energy. Nuclear and fossil fuels have adverse effects on the environment such as large amounts of greenhouse gases emissions and pollution from the burning of fossil fuel (René, 2005, Azhar and Abdul, 2012).

Since fossil fuel and nuclear sources of energy are not renewable, it is necessary to explore other sources of energy that are cost effective especially in the developing countries that rely heavily on imported fossil fuel. Renewable energy such as sunlight, wind tides and wave can be particularly suitable for developing countries especially in rural and remote areas where transmission and distribution of energy generated from fossil fuels can be difficult and expensive. Producing renewable energy locally can offer a viable alternative.

Technology advances are opening up a huge new market for solar power. There are approximately 1.3 billion people around the world who do not have access to grid electricity (*http://www.Renewable Energy in Developing Countries – wikipedia.Org*). Even though they are typically poor, these people have to pay far more for lighting than people in rich countries because they use inefficient kerosene lamps and stoves. Solar power costs half as much as lighting with kerosene. An estimated three million households get power from small solar panels (Duke *et al*., 2010).

Energy consumption in Kenya is in two areas, namely: in industries and for domestic purposes. Domestic consumption of energy is far much higher than industrial consumption. Hydro-electric power is largely used although it is not readily available especially in remote areas where there is no National Grid. Since Kenya is located along the equator where there is a vast expanse of sun's rays throughout the year, solar power provides a good alternative to supplement the energy demands.

Kenya is the world leader in the number of solar power systems installed per capita. More than 30 000 very small solar panels, each producing 12 to 30 Watts, are sold in Kenya annually (Duke *et al., 2010*).

In 2011, the International Energy Agency said that the development of affordable, inexhaustible, and clean solar energy technologies will have huge long-term benefits. It will increase a countries' energy security through reliance on an indigenous, inexhaustible and mostly import-independent resource, enhance sustainability, reduce pollution, lower the costs of mitigating climate change and keep fossil fuel prices lower (*http://www.Renewable energy in developing countries Wikipedia. Org).*

The energy conversion efficiency of a PV module or array as a group of electrically connected PV modules in the same plane is defined as the ratio between electrical power conducted away from the module and the incidence power of the sun (Rakovect *et al.,* 2011).

Solar cell conversion efficiency as a function of operating temperature is given as;

$$\eta_c = \frac{P_{\max}}{P_{in}} = \frac{I_{\max} \times V_{\max}}{I(t) \times A_c} \qquad (2.1)$$

where $I_{\max}$ and $V_{\max}$ is current and voltage for maximum power corresponding to irradiance ($I(t)$) and A_c is the area of the cell.

This conversion efficiency of photovoltaic (PV) modules by manufactures is done under Standard Test Conditions (STC). The Standard Test Conditions are module temperature of 25^o c, Irradiance of 1000W/m^2 and Air mass of 1.5).

The orientation of PV modules determines their power output. This orientation is described by its azimuth and tilt angle. For fixed modules, the azimuth angle is the angle the modules make with the true North, when measured in a clockwise direction. The tilt angle is the angle that forms between the horizontal and the long axis of the PV module. It is the latitude at a given location. Many investigations have been carried out to determine the best tilt angle for PV systems. Ibrahim, (1995) and Pavlovic *et al.,* (2010), suggests the following equation for optimum tilt angle (Φ).

$$\Phi = \left(\varphi \pm 15^o\right) \tag{2.2}$$

where φ is the latitude of a given place.

Different PV module technologies now exist in the market. These include crystalline modules such as mono/single crystalline, poly/multi crystalline and amorphous modules. The modules available are rated by manufacturer depending on their power output such as 5Watts, 10Watts, 15 Watts etc. The choice of the module to use depends on the power output needed by the consumer and its efficiency.

Photovoltaic (PV) modules are often considered as the most reliable elements in PV systems. However, PV module reliability data are not shown on commercial data sheets in the same way

as it is with other products such as electronic devices and electric power supplies. Conversely, the high reliabilities associated with PV modules are indirectly reflected in the output power warranties usually provided in the industry, which range from 25-30 years. As a matter of fact, PV modules have a very low total number of returns, the exceptions being the catastrophic failures. The performance of PV modules decreases when deployed outdoors over time. After several years of operation, this decrease will affect PV module reliability (Manuel and Ignacio, 2008).

2.2 Related Studies

Cornaro and Musella (2010) evaluated the performance of two PV modules, one polycrystalline and one amorphous during a medium term exposure at optimized tilt angle and did a complete characterization of weather conditions. The results showed that the polycrystalline module was highly stable with an average performance ratio (P.R) of 0.88. A seasonal trend in the monthly performance was observed due to the temperature effect on the module performance. The amorphous silicon module showed an effect of degradation in the first months of operation due to the Staebler- Wronski degradation effect.

Rong *et al*. (2011) reported that the degradation of solar photovoltaic modules is associated with the outdoor weather condition at the place of use.

Malik *et al.* (2010) studied the influence of temperature on the performance of photovoltaic polycrystalline silicon module in the Bruneian climate. I-V data was collected twice a week. Investigations on temporal variation (which includes variation in intensity of solar radiation, and its distribution of different components such as direct, diffused and global; ambient and working

temperature of the device) on the electrical performance of the devices was done. The results showed that polycrystalline modules worked well at low irradiance.

Carr (2005) performed a detailed comparison of PV modules of different technologies and their implications for PV system design methods in Australia. The experiments revealed that the STC values quoted by the manufacturers for the PV modules do not necessarily match those observed in STC measurements.

Osterwald *et al.* (2002) performed a degradation analysis of four different weathered crystalline silicon PV modules by exposing them to real time outdoors at fixed tilt. It involved accelerating outdoors at global normal irradiance and three times mirror enhancement (outdoor accelerated-weathering test system, OATS). The results showed that there was a linear relationship between maximum power degradation and the total ultra violet exposure dose for the four different types of modules. Analysis of data from long term solar weathering study revealed a slow *Isc* degradation which begun after the rapid initial light–induced degradation caused by oxygen contamination in boron-doped Si solar cells.

Agroui *et al*. (2011) evaluated the indoor and outdoor photovoltaic modules performances based on thin films solar cells. The tests showed that the STC values quoted by manufacturers for their amorphous modules do not match those observed in STC measurements. The modules were found to degrade within the first 8-10 weeks of exposure due to Staebler-Wronski effect on the amorphous silicon material.

Siddiqui *et al*. (2014) performed an analysis of polycrystalline silicon PV modules on the basis of indoor and outdoor conditions. The results showed that the STC values quoted by

manufacturers for their multi crystalline silicon PV modules do not necessarily match those observed in STC measurements.

Duke *et al*. (1999) conducted a survey on the field performance of amorphous Silicon (a-Si) photovoltaic modules in Kenya. The research revealed that small 10 to 14 Watt single junction amorphous Silicon (a-Si) modules dominate the market. Despite the commercial success there is substantial concern about the performance of single junction thin films amorphous silicon (a-Si) both because of the technologies uneven quality and the uncertainty introduced by short term degradation which occurs when this type of PV module is initially exposed to the sun.

A survey conducted by Duke *et al*. (2010) indicates that only 9% of PV module consumers think they know the brand of the modules they owned, and 15% of these respondents answered incorrectly. In addition, over 40% of the respondents would not guess about how long their modules would last. Less than 3% of the respondents knew whether they had an amorphous or crystalline solar module and only 6% of the respondents had an opinion about whether amorphous or crystalline modules existed.

CHAPTER THREE

THEORITICAL BACKGROUND

3.1 Overview of Photovoltaic Technologies

A wide range of photovoltaic technologies now exist in the market which include crystalline silicon (c-Si) and thin film technologies of amorphous silicon. The crystalline silicon (c-Si) includes single-crystalline silicon and multi-crystalline silicon. Thin-film technologies include amorphous silicon (a-Si), micro morph (micro-crystalline/ amorphous silicon), cadmium telluride (CdTe) and copper-Indium-gallium-diselenide (CIGS). Each technology is mainly described and classified according to the material used, manufacturing procedure and efficiency. Amongst the various existing PV technologies, crystalline silicon is the most developed. Silicon at present is the most abundant material found in the earth's crust and its physical properties are well defined and studied. C-Si dominates the PV technology market with a share of approximately 80% (Makrides *et al*., 2010).

The main characteristic of mono-c-Si is its ordered crystalline structure with all the atoms in a continuous crystalline lattice. Mono-c-Si technologies are highly efficient but are at the same time the most expensive amongst the existing PV technologies mainly because of their relatively costly manufacturing processes. The substrate thickness is about 400-200 μm and increased the surface area from 100cm^2 to 240cm^2. The thickness should be approximately 200 μm to allow incident light to be absorbed within a wide range of wavelengths.

Multi-c-Si solar cell wafers consist of small grains of mono-c-Si and are made in a number of manufacturing processes. The substrate thickness is approximately 160 μm while attempts are being made to lower the thickness even more. In general multi-c-Si PV cells are cheaper

compared to mono-c-Si as they are produced in less elaborate manufacturing process, at the expense of slightly lower efficiencies. The lower efficiency is attributed to recombination at the grain boundaries within the multi-c-Si structure.

Ribbon silicon is another type of multi-c-Si technology which is produced from multi-c-Si suitable for the photovoltaic industry. In the manufacturing process of this technology, high temperature resistant wires are pulled through molten silicon to form a ribbon which is subsequently cut and processed in the usual manner to produce PV cells. An advantage of this technology is that the production cost is lower than other c-Si technologies, while the efficiency and quality of the cells remain the same as other multi-c-Si technologies but lower than mono-c-Si.

The main incentive for the development of thin film technologies has been their cheap production cost compared to the c-Si counterparts. Over the past years, thin-film technologies have shown very encouraging development as the global production capacity has reached around 3.5GW in 2010 and is expected reach between 6-8.5GW in 2012 (Makrides *et al*., 2010). Amongst the many thin-film technologies some of the most promising are CdTe, a-Si, micro morph tandem cells (a-Si, μ c-Si) and CIGS.

Amorphous silicon has been on the PV market longer than other thin-film technologies and this has allowed researchers and manufactures to understand several aspects of its behavior. This technology was first commercialized in the early 1980's and since then has increased gradually in efficiency (*Duke et al*., 1999). The manufacturing of a-Si technologies is dominated by deposition processes such as plasma enhancement chemical vapour deposition (PECVD) and

thus large area, flexible and cheap substrates such as stainless steel and thin foil polymer can be used.

In comparison to mono-c-Si, amorphous silicon PV cells have no crystalline order, leading to dangling bonds which have severe impact on the material properties and behavior. Another important material limitation arises from the fact that this technology suffers from light-induced degradation, known as Staebler-Wronski effect (SWE). SWE describes the initial performance decrease when a-Si modules are first exposed to light (Agroui *et al*., 2011). In general, the effect has been minimized by employing double or triple-junction devices and developing micro morph tandem cells, which is a hybrid technology of c-Si and a-Si. An important advantage of a-Si is the high absorption co-efficient which approximately 10 times higher than c-Si therefore resulting in much thinner cells.

The concept of micro morph (micro crystalline/ amorphous silicon) tandem cells was introduced to improve the stability of a-Si tandem cells. The structure of micro morph device has a-Si cell which is optimized with the application of the micro-crystalline silicon (μc-Si) layer of the order of $2\,\mu$m onto the substrate. The application of the μc-Si layer assists the device in increasing its absorption in the red and near infrared part of the light spectrum and hence increases the efficiency by up to 10%.

Another type of thin film technology is CdTe, which is a group II- VI semiconductor with a direct band gap of 1.45eV. The high optical absorption co-efficient of this technology further allows the absorption of light by a thin layer as it absorbs over 90% of available photons in a $1\,\mu$m thickness hence films of only 1-3 μm are sufficient for thin-film solar cells. CdTe technology is a front-runner amongst thin-film PV technologies due to the fact that it can be

produced relatively cheaply and module efficiencies have reached 12.8%. So far, the achieved efficiency of this technology is lower compared to c-Si, but higher than triple-junction a-Si. In comparison to a-Si, the CdTe PV technology does not show initial degradation. In addition, the power is not affected to the same extent by temperature variations as c-Si based technologies.

The table 3.1 gives a summary of different commercial PV module technologies, their different film thickness; the range of their efficiencies and their surface area of summarizes the key characteristics of typical commercial PV modules.

Table 3.1: Typical commercial PV Module Characteristics (Makrides et al., 2010)

Technology	Material thickness (μm)	Area (m^2)	Efficiency (%)	Surface area for 1KWp system(m^2)
Mono-c-Si	200	1.4-1.7(typical)	14-20	≈ 7
multi-c-Si	160	1.4-1.7(typical)	11-15	≈ 8
a-Si	1	1.5	4-8	≈ 15
a-Si/ μ c-Si	2	1.4	7-9	≈ 12
CdTe	≈ 1-3	≈ 0.6-1	10-11	≈ 10
CIGS	≈ 2	≈ 0.6-1	7-12	≈ 10

3.2 Outdoor and Standard Test Condition (STC)

The performance of silicon solar cells are affected on changing the environmental factors. Solar cells, like all other semi-conducting materials are subjected to electrical degradation. Solar cells

are exposed to temperatures changing from 10 degrees to 50 degrees Celsius. The output parameters like open circuit voltage, fill factor, short circuit current and efficiency of the solar cells are temperature dependent (Singh *et al*., 2011). In evaluating PV performances in outdoor operating conditions, for practical use, it is difficult to create the measurement conditions identical to standard test conditions (STC) which are irradiation intensity of 1000 W/m^2, module temperature of 25^{o}C and air mass 1.5 (Singh *et al*., 2011).

The I-V curves obtained outdoors therefore are normalized to standard test condition using the normalizing equation 3.1 and 3.2 according to Malik *et al*., (2010).

$$I_n = I_n \times \frac{1000W/m^2}{E} \tag{3.1}$$

where I_n is the normalized current, I_m is the measured current outdoors and E is the measured irradiance.

$$V_n = V_m \times \{1 + b(25^oC - T)\} \tag{3.2}$$

where V_n is normalized voltage (Volts), V_m is measured voltage (Volts), b is the temperature coefficient (V/ ^{o}C) and T is the module temperature (^{o}C).

3.3 Photovoltaic Performance Parameters

The electrical properties of a PV device comprises of: open circuit voltage (V_{oc}), the short circuit current (I_{sc}), maximum voltage (V_{max}), maximum current (I_{max}), maximum power (P_{max}),

conversion efficiency (η), and fill factor (FF). Some of these parameters are measured by the manufactures at standard test conditions (STC).

Solar cells only convert a small amount of absorbed solar radiation into electrical energy. The excess incident energy is dissipated as heat in the bulk of the silicon solar cell which increases its temperature compared to the environmental conditions. An increase in the working temperature of a solar cell reduces the band gap allowing more energy to be absorbed which increases the short circuit current (I_{sc}) of the solar cell for a given irradiance.

The band gap energy $E_g(T)$ of the material as a function of temperature can be written as;

$$E_g(T) = E_g(0) - \frac{aT^2}{T+b} \tag{3.3}$$

where $E_g(0)$ is the band gap energy of the material at room temperature; a and b are constants. This effect alone raises the theoretical maximum output power of the solar cell. At the same time an increase in the temperature increases the population of electrons exponentially. This enhances the dark saturation current (I_O) that is a minority carrier current and its variation with temperature can be written as in equation 3.4;

$$I_0 = A_0 T^3 \exp\left(-\frac{E_g}{K_B T}\right) \tag{3.4}$$

where A_o and K_B are the area of the device and Boltzmann's constant. The increase in the dark saturated current decreases the open circuit voltage (V_{oc}) of the device that is expressed in equation 3.5;

$$V_{oc} = \frac{K_B T}{e} \ln\left(\frac{I_{sc}}{I_0} + 1\right) \tag{3.5}$$

Theoretically, a decrease in the open circuit voltage would reduce the output power of the device. The short circuit current and the open circuit Voltage are related to an important property of a PV device known as the fill factor (*FF*) which is defined as the ratio of the of the maximum power of the PV device to the product of I_{sc} and V_{oc} as indicated in equation 3.6;

$$FF = \frac{V_{\max} I_{\max}}{V_{oc} I_{sc}} \tag{3.6}$$

The fill factor diminishes as the temperature of the device is increased. The decrease in V_{oc} and fill factor (*FF*) with the working temperature of the device outweighs the slight increase in the short circuit current.

3.3 Effect of Temperature on PV Performance

Jefari *et al*. (2011) reported that Solar cells performance parameters vary due to temperature changes. The change in temperature will affect the power output from the cells. The voltage is highly dependent on the temperature and an increase in temperature will decrease the voltage. Figure 3.1 shows the effect of temperature on I-V characteristics of PV module at constant radiation. As the temperature of the module is increased from 10^{o}C to 70^{o}C the short circuit current of the module decreased slightly while the open circuit voltage decreased significantly from 25V to 18V.

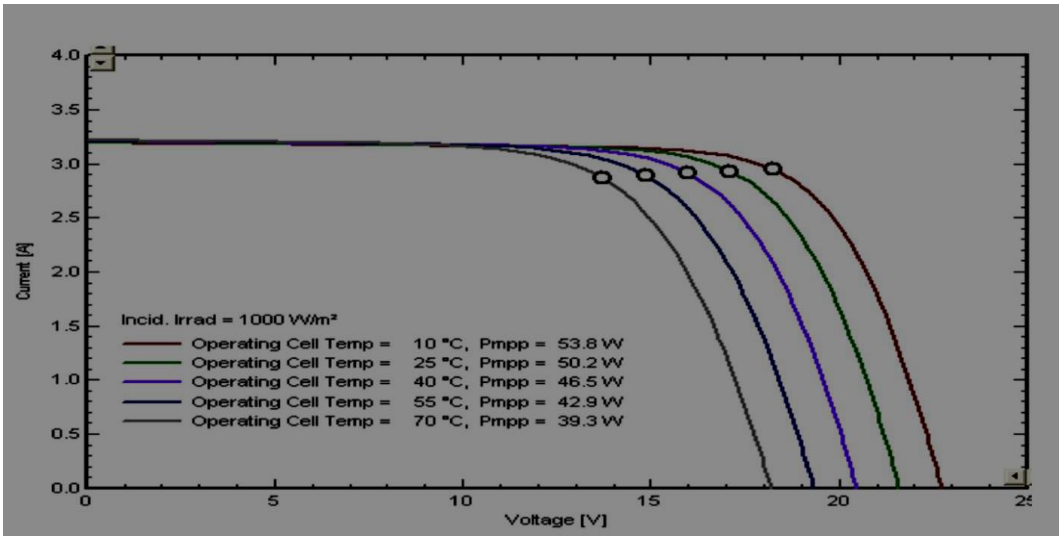

Figure 3.1: Output I-V characteristic of the PV modules with different temperature Jefari *et al*. (2011)

More than 80% of solar radiation reaching the photovoltaic cell (PV) is not converted into electricity. It is reflected or transformed into heat energy. The heat generated yields to an increase in cell temperature and consequently to a decrease in conversion efficiency of the cell. Thus as the cell temperature is increased, the output power of the cell decreases significantly as shown in figure 3.2.

3.4 Standard Rating of PV Modules

In comparing different modules the standard rating system used is a peak power value given by manufacturers. This is based on the module maximum power output at standard test condition (STC). The standard test condition is an irradiance of 1000W/m^2 at air mass AM 1.5 and a cell or module temperature of 25^{o}C. Generally, the information supplied by photovoltaic (PV) manufacturers includes the following parameters: P_{max}, V_{oc}, I_{sc}, V_{mp} and I_{mp}.

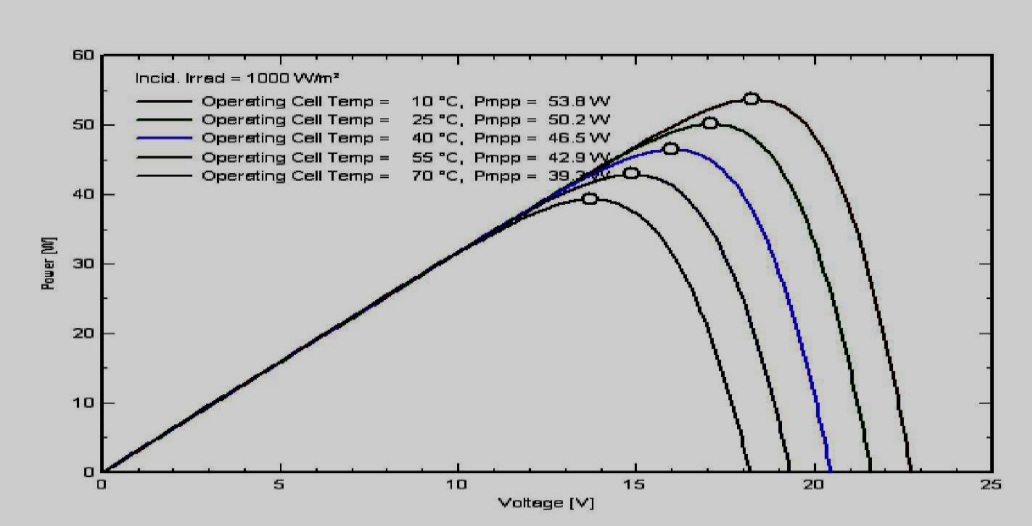

Figure 3.2: Output characteristics of the PV module with different temperature Jefari *et al*. (2011)

Another value often supplied by manufacturers is the Nominal Operating Cell Temperature (NOCT). It is defined as the cell temperature of an open-circuited, rack-mounted module at standard test operating condition (SOC). SOC represents a more realistic operating condition for a PV module than STC. SOC is defined as an irradiance of 800W/m^2, an ambient temperature of 20^{o}C and a wind speed of 1m/s. By providing the NOCT value a user or a system designer can calculate a thermal capacitance value for the module and thereby estimate cell temperature at other operating conditions. Occasionally, manufacturers give voltage and current values at SOC. At other occasions they do provide temperature coefficients either for V_{oc} and I_{sc} or for P_{max}.

The size attributed to a PV array is calculated from this STC W_p (peak-Watt) rating, even though the standard test conditions described above are rarely experienced by modules under actual operation. A 20kW array, for example, consists of an array of PV modules whose W_p rating totals 20k Watts, though, depending on the location, it is highly unlikely the array will ever produce a power of 20kW. The SOC and NOCT values provide more realistic indication of the

output of the modules under actual operation, but, these are ideal conditions and not a representative of the full range of operating conditions.

3.5 Failure Modes of PV Modules

To survive in harsh operating environmental conditions, PV modules rely on packaging materials including protective superstrate, substrate, sealants and encapsulants to provide requisite reliability. Several key properties associated with PV module reliability are critical for commercial success. These include:

i. Low-interface conductivity

ii. Adequate adhesion of encapsulants to substrate, superstrate and PV cells

iii. Low moisture permeation through all packaging materials and

iv. Good mechanical properties such as tensile elongation and creep resistance at all operating conditions.

Therefore, it is important to investigate how properties changes and or degradation in polymetric materials used in PV modules and understand the correlation among materials degradation and failures of PV module system performance in the field. Figure 3.3 illustrates the failure modes of PV modules caused by packaging materials degradation under multiple stresses including heat, moisture and UV (Ethan and Edwin, 2012). The suggested evaluating approaches for these modes are also specified.

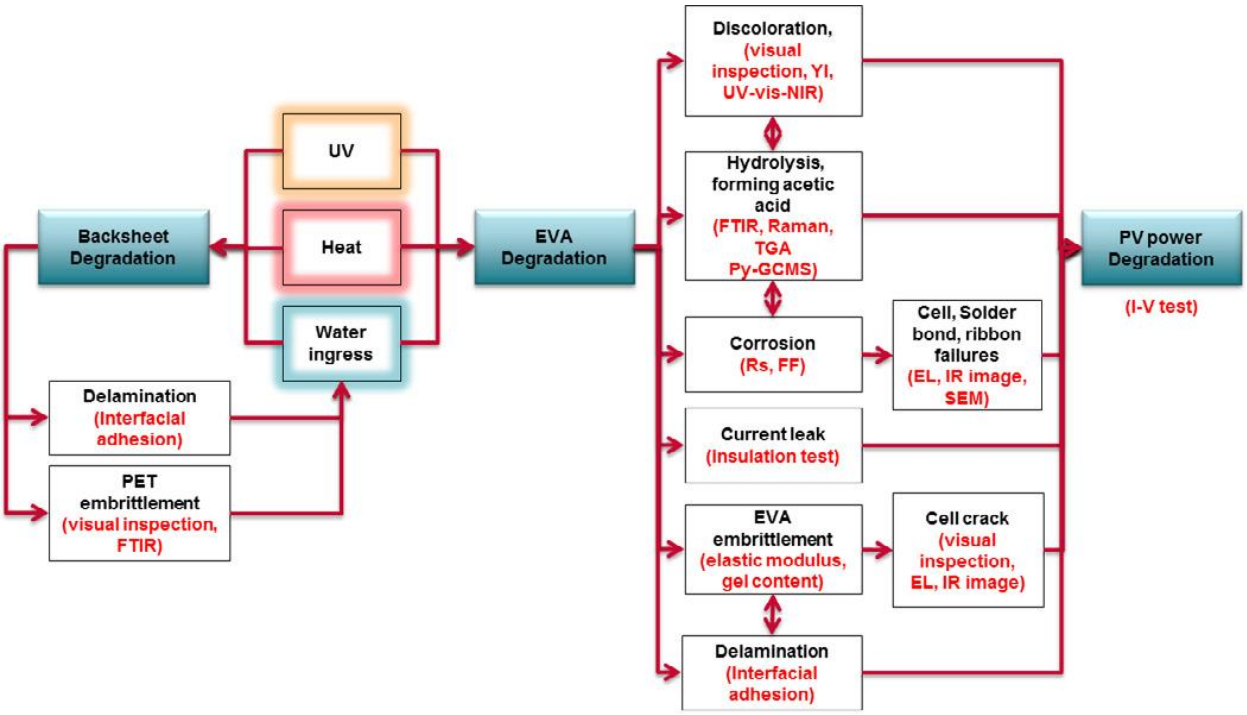

Figure 3.3: Failure modes of PV modules caused by packaging materials and the evaluating approaches (Ethan and Edwin, 2012)

3.6 Determining the Optimum Angle of Tilt for the Modules

In order to have maximum sunlight converted into usable energy, the tilt angle of the PV surface should be maximized. This is due to the fact that tilt and orientation of PV surface determines the amount of electricity that can be generated. The PV surface should be positioned in a way that its plane of array is directly perpendicular to the sun's rays for a longer duration. This will capture the maximum amount of sunlight to be converted (Prashanthini *et al.,* 2011 and Pavloc *et al*., 2010).

The orientation of a solar collector is described by its azimuth and tilt angles. Systems installed in the northern hemisphere are oriented toward south and tilted at a certain angle. The azimuth angle is the angle the panels make with the true north, when measured in a clockwise direction. In the northern hemisphere this angle is 180^{o}, which makes the panel to face south. For installations in the southern hemisphere, this will be zero degrees making the panels to face

north. The tilt angle is the angle that is formed between the horizontal and the long axis of the PV module. It tells how much the panel should be tilted to derive the best incidence of solar energy.

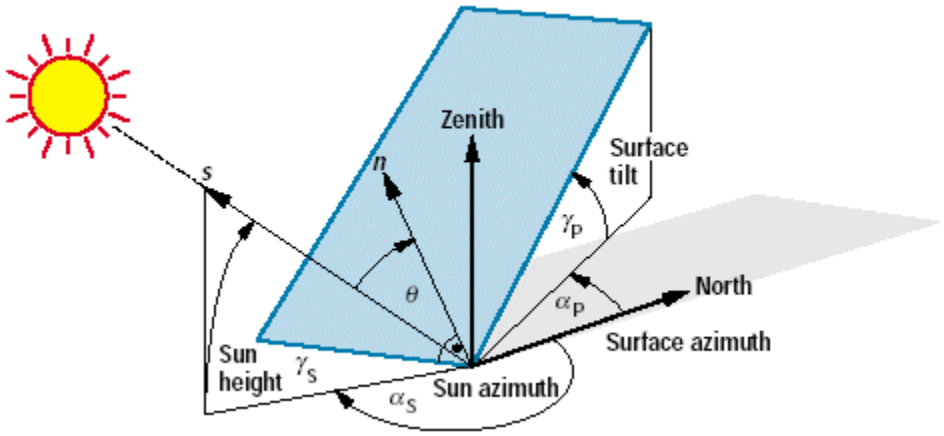

Figure 3.4: Angle of tilt of a PV module

Equation 3.7 was used to determine the optimal angle of tilt to be used in this study (Kacira *et al*., 2004; Prashanthini *et al*., 2011).

$$\Phi = \left(\varphi \pm 15^{o}\right) \tag{3.7}$$

where φ is the latitude of the location. Plus (+) sign is used in winter and the minus (-) sign in summer. In this work the modules were placed at a fixed angle of tilt of 15 degrees, which is the angle that receives most irradiance.

.

CHAPTER FOUR

MATERIALS AND METHODS

4.1 Description of the Work Done

This study was investigating the performance of nine photovoltaic modules three mono crystalline, polycrystalline and amorphous types. The modules were placed at a fixed angle of tilt of 15 degrees since it is the angle that receives most irradiance. The I-V data was measured every day at solar noon since this is the time the irradiance in a day is maximum. The data was measured from the months of August to November. Due to changes in irradiance while collecting data, the irradiance was measured in the beginning and at the end of collecting data for each module. The ambient temperature and back of the module temperature was measured at the beginning and the end of data collection for each module. Finally an average of irradiance and temperature was calculated and used for the various calculations. The collected data was normalized to Standard Test Conditions and then the I-V curves were drawn using the normalized data. From the I-V curves, parameters such as I_{sc}, V_{oc}, I_{max}, and V_{max} were read and parameters such as P_{max}, efficiency and Fill Factor (FF) of the modules calculated. Graphs of these parameters against days of exposure were plotted. The gradient of the graph represents the rate of degradation of each module parameter

4.2 Experimental Set Up

The initial I-V data of the nine silicon based modules (mono crystalline, poly-crystalline of 10W, 15W and 20W respectively and amorphous of 10W, 15W and 18W) form different manufacturers was measured at an angle of inclination of 15degrees to determine the initial

parameters. The modules were then mounted on a fixed angle rack. Visual inspection of the modules was also done before they were mounted.

Figure 4.1 shows the nine modules mounted at a fixed angle of tilt of 15 degrees. This is the optimal angle that receives most irradiation.

Figure 4.1: Experimental set up

4.3 The I-V Curve Trace Meter

I-V data was collected using a I-V curve trace meter. Using equations 3.1 and 3.2, the collected I-V data was normalized to standard test conditions (STC). Figure 4.2 shows the Current-Voltage (I-V) curve trace meter that was used in data collection. The shunt resistor used was of 0.0667 Ohms prepared by arranging three 0.2 Ohm resistors in parallel. The Voltage across the shunt resistor was measured and current calculated using relation 4.1;

$$I_{sh} = \frac{V_{sh}}{R_{sh}} \tag{4.1}$$

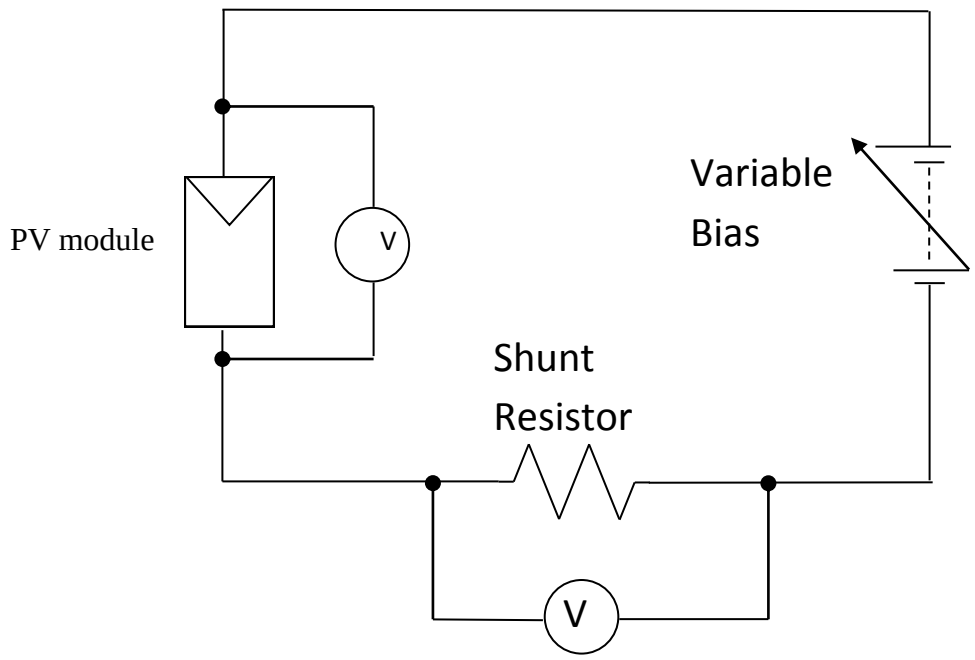

Figure 4.2: I-V curve tracer showing variable bias and shunt resistor

Using the STC normalized I-V data; I-V curves of various modules were plotted.

To extract the solar cell device and performance parameters, the normalized I-V data was modeled using the one-diode model.

The performance parameters of different modules were then compared.

4.4 A Pyranometer

A pyranometer was used to measure the solar irradiance for various I-V data.

Graphs of V_{oc} ,I_{sc}, P_{max} and efficiency against the number of days for each module were drawn to examine each module's degradation rate.

Figure 4.3: Photograph of a CM3 pyranometer

4.5 Conversion of Obtained Values to Standard Test Conditions (STC)

Since the outdoor conditions experienced by the modules are different from the Standard Test Conditions (STC) used by manufacturers while quoting the performance of the modules, the obtained values were normalized to STC using equations 3.1 and 3.2.

4.6 Module and Ambient Temperature Measurement

The temperature of the modules and the ambient temperature for each of the I-V curves were measured using a thermocouple. In order to correct recorded data to STC the ambient temperature played a very important role. A thermocouple is a sensor for measuring temperature. It consists of two dissimilar metals joined together at one end. When the junction of the two metals is heated or cooled a voltage drop is produced proportional to temperature.

4.7 Visual Inspection of the Modules

Photovoltaic (PV) modules can degrade on different accounts (Manuel *et al*., 2008).These include the technology of the modules such as if they are mono crystalline, polycrystalline or amorphous and the location of use (temperature, humidity and radiation). PV modules can degrade their performance as a result of different factors such as:

i. Degradation of packaging materials

ii. Loss of adhesion of encapsulants

iii. Degradation of cell/ module interconnection

iv. Degradation caused by moisture intrusion

v. Degradation of the semiconductor material

In the case of crystalline Si PV modules, the degradation of the semiconductor is not important because of the stability of the semiconductor material. Field experience indicates that the primary causes of performance losses are associated with mechanisms external to the cell itself such as solder joints, encapsulant browning, delamination and interconnection problems.

Visual inspection of the modules was done every day by carefully inspecting them. Photographs of the modules were taken when a change in the module was noticed.

4.8 One-Diode Solar Cell Model

The model assumed in this work is the one-diode model. Figure 4.4 presents the electrical scheme of this model.

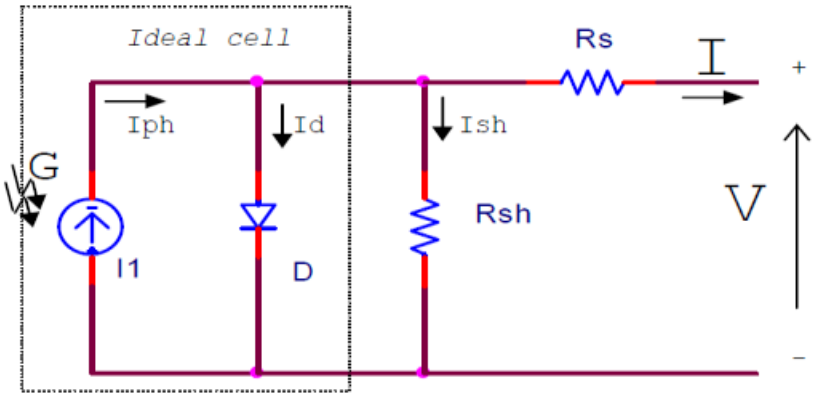

Figure 4.4: One diode equivalent circuit model of a solar cell

In practice solar cell is not an ideal diode so there are some losses. In real cells the parasitic effect is due to the presence of series resistance R_s and parallel resistance R_{sh}. Series resistance R_s is very small which arises from the Ohmic contact between metal and semiconductor internal resistance (Abdul *et al*., 2012). The shunt resistance is very large and represents the surface quality along the periphery. Leakage current through the periphery represents I_{sh}. Both the diode current I_d and shunt current I_{sh} are from the photocurrent I_{ph}. In an ideal case the R_s is 0 and the R_{sh} is ∞. The resultant current relationships are in the following equations as dictated by Kirchhoff's current laws.

$$I = I_{ph} - I_d - I_{sh} \tag{4.2}$$

The current being sent through the diode is;

$$I_d = I_o(\exp \frac{V_d q}{AKT_c} - 1) \tag{4.3}$$

Where q is the electron charge = 1.60 $\times 10^{-19}$ Coulombs, K is the Boltzmann constant = 1.38 $\times$ 10^{-23} joules/ kelvin, A is the diode ideality factor (manufacturing value is between 1 and 2), T_c is the

cell temperature, Io is the saturation current and V_d is the voltage across the diode. The diode voltage V_d is given by equation 4.4;

$$V_d = IR_s + V \tag{4.4}$$

Equation 4.2 can therefore be re-written as shown in equation 4.5;

$$I = I_{ph} - I_o\left[\exp\frac{(V + IR_s)q}{AKT_c} - 1\right] - \frac{V + IR_s}{Rsh} \tag{4.5}$$

When the terminals of a solar cell are open circuited the photocurrent generated by the current source fully flows through the diode and R_{sh} and the maximum voltage V_{oc} is produced across the terminal. When considering the case that the terminal of the photovoltaic cell is short circuited the photocurrent I_{ph} flows through the short circuited terminal and so the voltage across the terminal become zero and current I_{sc} become I_{ph}. So the short circuit current I_{sc} is equal to I_{ph}. Then current I can be written as shown in equation 4.6;

$$I = I_{sh} - I_o\left[\exp\frac{IR_s + V}{AKT_c} - 1\right] - \frac{V + IR_s}{R_s} \tag{4.6}$$

I_{sc} depends on weather conditions such as ambient temperature (T_a) and irradiance G as indicated by equation 4.7;

$$I_{sc} = \frac{G}{1000}\left(Iscr + Ki(Tc - Tr)\right) \tag{4.7}$$

where, T_r is the temperature in kelvin at STC, T_c is the cell temperature in kelvin, I_{scr} is the short circuit current at STC, K_i is the temperature coefficient and G is the solar irradiation in Watts/m^2.

The cell temperature is a function of ambient temperature (T_a) and irradiation G given by equation 4.8;

$$T_c = \frac{NOCT - 20}{0.8} G + T_a \qquad (4.8)$$

where, $NOCT$ is the nominal operating cell temperature.

When I =0, then the output voltage is termed as the open circuit voltage V_{oc} given by equation 4.9;

$$Voc = \ln(\frac{Isc}{Io} + 1)(\frac{AKTc}{q}) \qquad (4.9)$$

4.9 Fill Factor (FF)

The Fill Factor (FF) is a measure of quality of the solar cell. It is calculated by comparing the maximum power to the theoretical power (P_T). FF can also be interpreted graphically as the ratio of the rectangular areas depicted in figure 4.5.

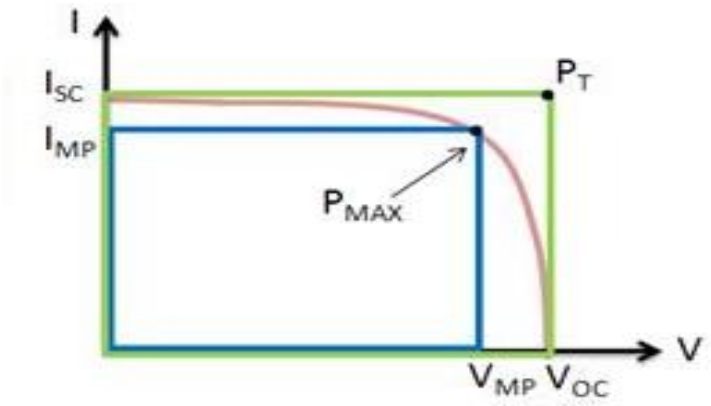

Figure 4.5: Schematic illustration of I-V sweep curve showing P_{max}, V_{oc}, I_{sc} and I_{mp}

A larger fill factor (approximately = 1) is desirable, and corresponds to an I-V sweep that is more square-like. Typical fill factors range from 0.5 to 0.82 (http://www.Solmetric.com, 2011). Fill factor is also often represented as a percentage.

4.10 Efficiency (η)

Efficiency is the ratio of the electrical power output (P_{out}), compared to the solar power input (P_{in}), into the PV cell. P_{out} can be taken to be P_{MAX} since the solar cell can be operated up to its maximum power output to get the maximum efficiency.

$$\eta = \frac{P_{out}}{P_{in}} \Rightarrow \eta_{MAX} = \frac{P_{MAX}}{P_{in}} \tag{4.10}$$

P_{in} is taken as the product of the irradiance of the incident light, measured in W/m^2 or in suns (1000 W/m^2), with the surface area of the solar cell [m^2].

CHAPTER FIVE

RESULTS AND DISCUSSION

5.1 Determination of the Temperature Co-efficient

While determining the V_{oc} and I_{sc} temperature co-efficients, one module from each technology was selected i.e. mono crystalline, polycrystalline and amorphous. The I-V curves of each module type were collected at cell temperatures ranging between 10 – 25 degrees Celsius. The I_{sc} and V_{oc} values were read from the curves and graphs of V_{oc} against temperature and I_{sc} against temperature were drawn. The slope of the graphs of each module type was generalized to the other three modules of the same kind and the parameters α and β were determined. Where α is the voltage temperature coefficient and β is the current temperature coefficient.

Table 5.1: Temperature coefficients

Module type	α	B
Mono crystalline	-0.0428	0.0467
Polycrystalline	-0.0329	0.023
Amorphous	-0.0712	0.0175

The obtained values were found to agree well with those found in literature (Ryan M. *et al*., 2012).

5.2 Obtained Module Performance Parameter

5.2.1 Measured V_{oc}

The open circuit voltage (V_{oc}) of a cell is the voltage of the cell when the current is zero. From the obtained results, the V_{oc} was found to have undergone degradation within the first four months of exposure. The amorphous module type registered a higher degradation of V_{oc} compared with the mono crystalline and the polycrystalline module types. This was attributed to a large layer of dust that covered the module as indicated in figure 5.4. Figure 5.1 shows variation of V_{oc} with the number of days of exposure. From the graph a gradual drop in V_{oc} is observed. The 10W mono crystalline was found to degrade faster as compared to 20W and 15W modules.

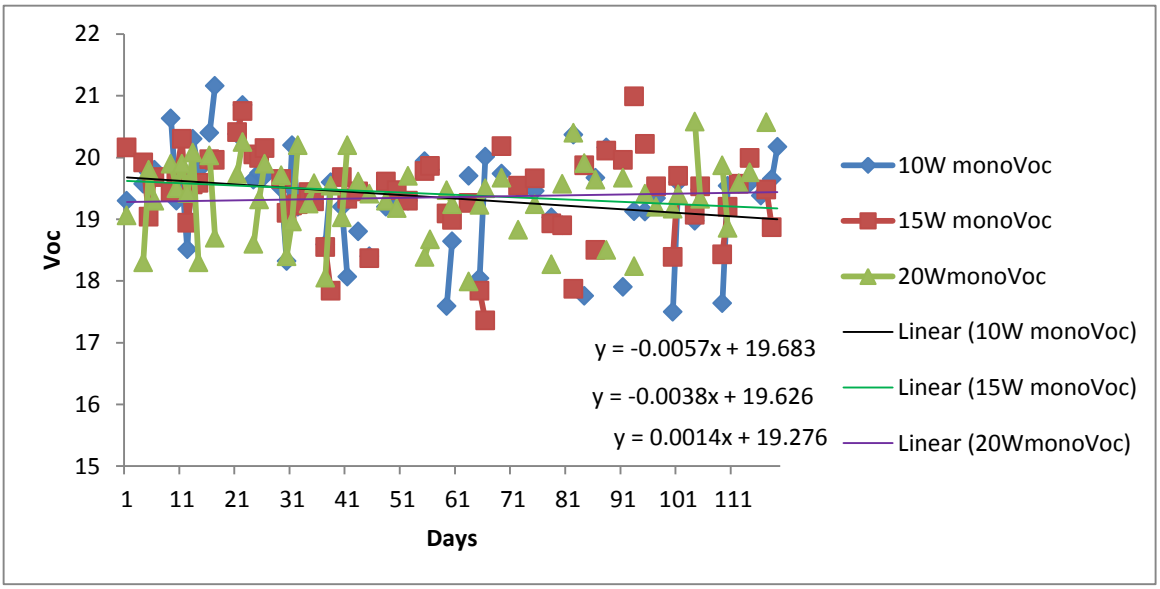

Figure 5.1: Graph of normalized V_{oc} against number of days for the mono crystalline modules

Figure 5.2 shows normalized graphs of V_{oc} against time for polycrystalline modules. From the graphs it can be observed that there is general drop in V_{oc} for all the modules. 10W polycrystalline module has a higher drop.

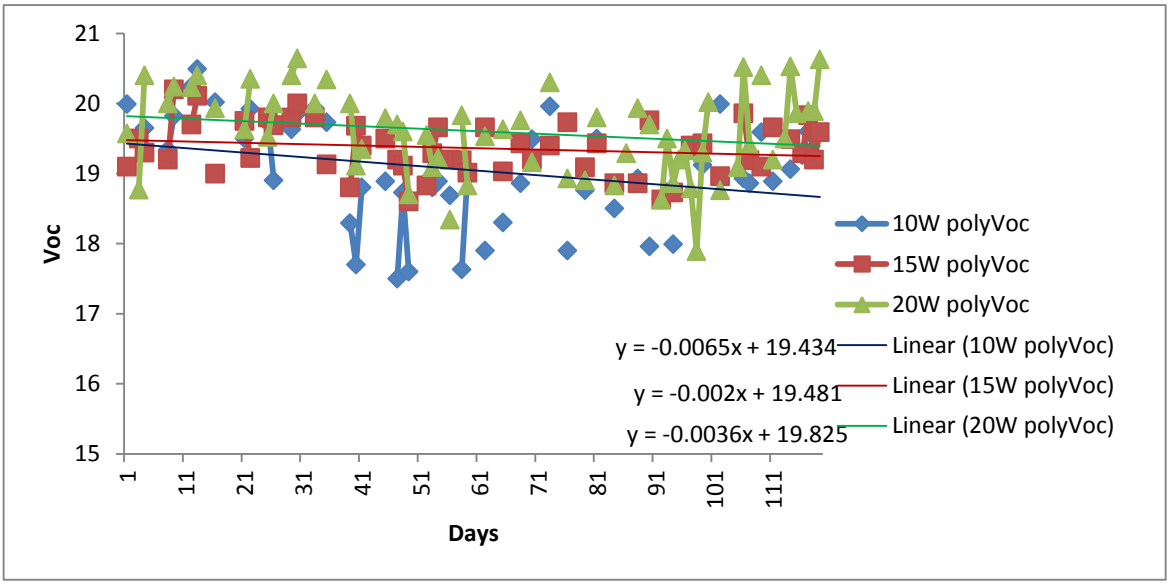

Figure 5.2: Graph of normalized V_{oc} against number of days for the polycrystalline modules

Figure 5.3 shows graphs of V_{oc} against number of days for the amorphous modules. From the graphs it is observed that the V_{oc} of the amorphous modules experienced the Staebler-Wronski degradation effect within the first thirty days of employment.

Figure 5.4 is a graph of Voc for amorphous modules against the first forty days of exposure. From the graph it is noted that the modules experienced the Staebler-Wronki effect. This is the degradation mechanism that occurs when amorphous silicon is first exposed to sunlight.

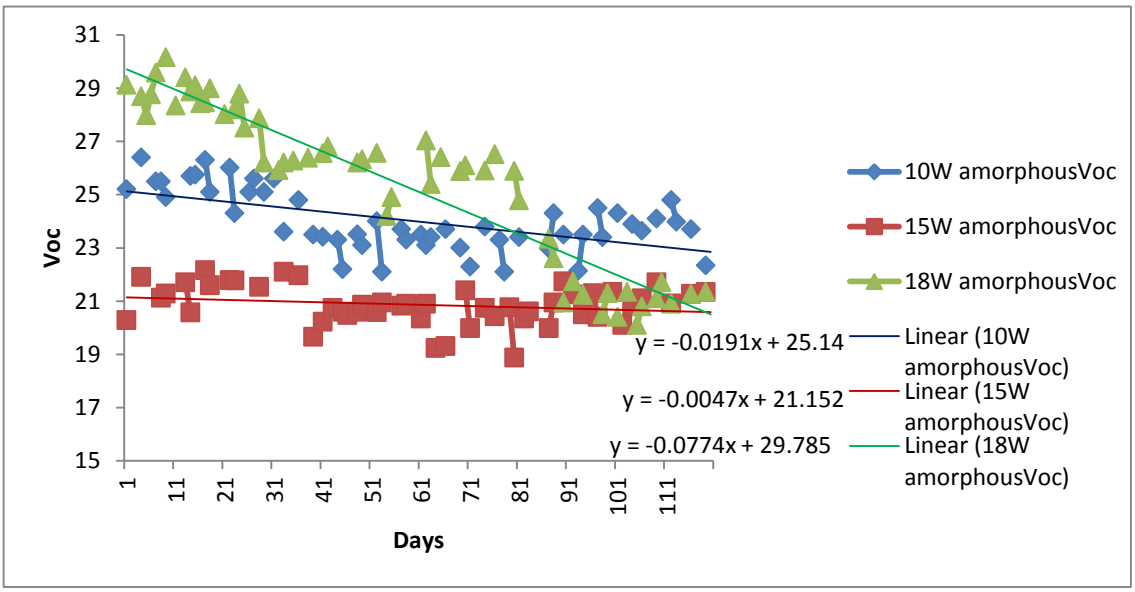

Figure 5.3: Graph of normalized V_{oc} against number of days for the amorphous module type

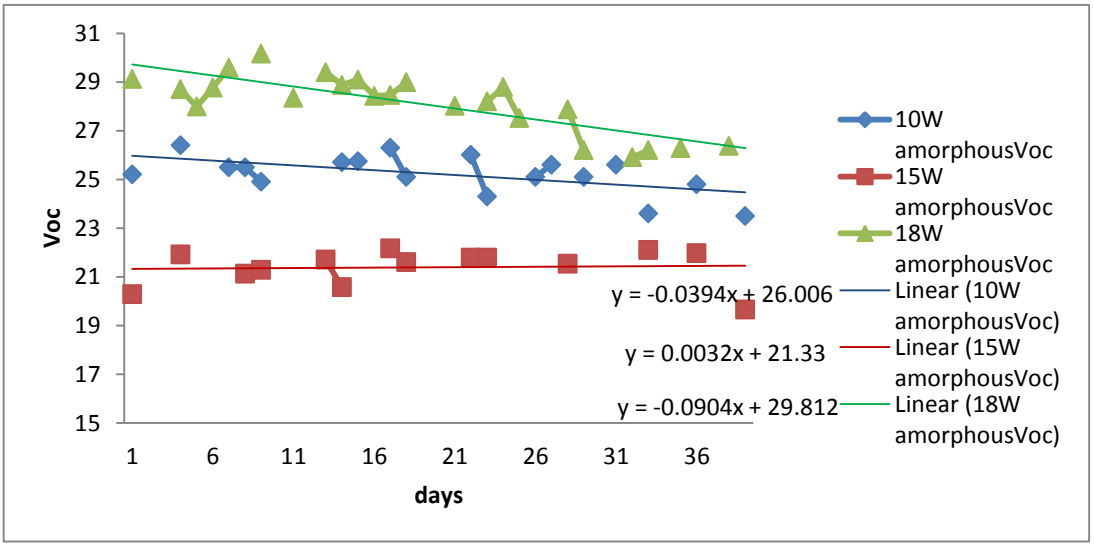

Figure 5.4: Graph showing the Staebler-Wrosnki Effect on V_{oc} of the amorphous module

Figure 5.5 is a graph of V_{oc} against number of days for amorphous modules after Staebler-Wronski Effect. It is noted that the 10W and 15W modules shows stability after forty days of

exposure while the 18W module does not. This shows that apart from the degradation as a result of first exposure, the 18W module continues to experience reduction in V_{oc} as a result of the layer of dust that is continuing to increase covering more cells.

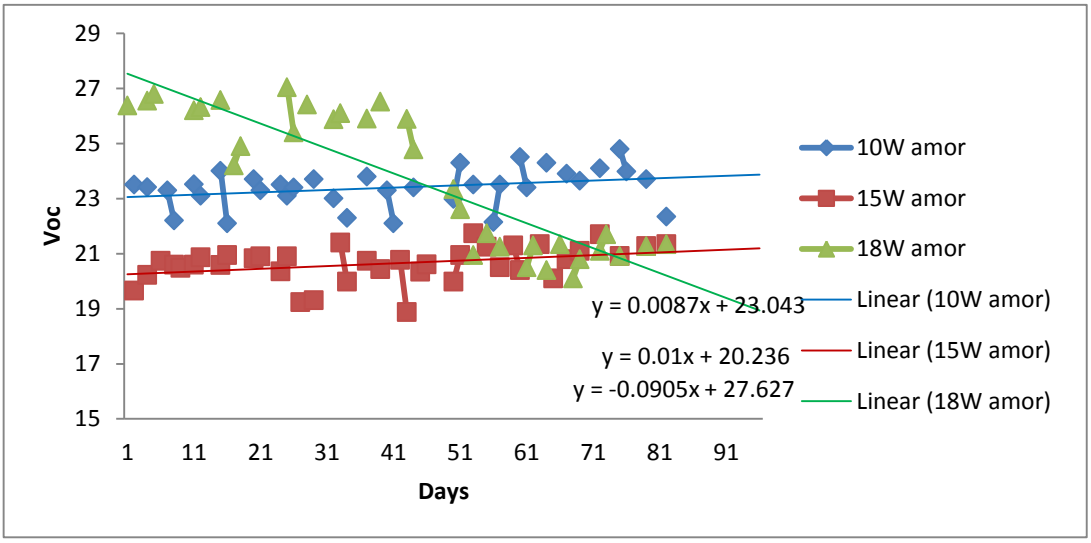

Figure 5.5: Graph of V_{oc} against days for the next eighty days after Steabler-Wronski degradation

Figure 5.6 shows the 18W amorphous modules covered by a large layer of dust. This module had a higher drop in V_{oc} compared with the other amorphous modules since a large portion of its cells were shaded by the dust particles. It was possible to clean the modules with water so that their output is not interfered with but this was not done since most of the module consumers in Kenya do not clean their modules once they mount them outside. The modules were therefore allowed to experience the real outdoor conditions.

Figure 5.6: 18W amorphous module type showing a portion of cells covered by a thick layer of dust

5.2.2 Measured Short Circuit Current (I_{sc})

Figure 5.7 is a graph of I_{sc} against number of days for the mono crystalline modules. From the graphs it is noted that there is negligible change in I_{sc} for the three mono crystalline modules.

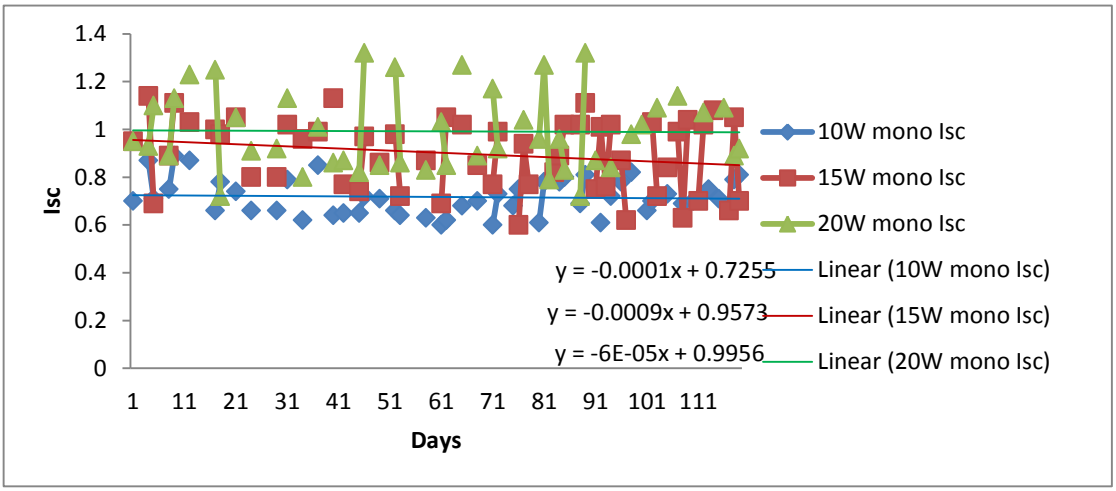

Figure 5.7: Graphs of normalized I_{sc} against number of days for the mono crystalline modules

Figure 5.8 is a graph of I_{sc} against number of days for the polycrystalline modules. From the graphs it can be seen that there is very little change in I_{sc} with the number of days for the polycrystalline modules.

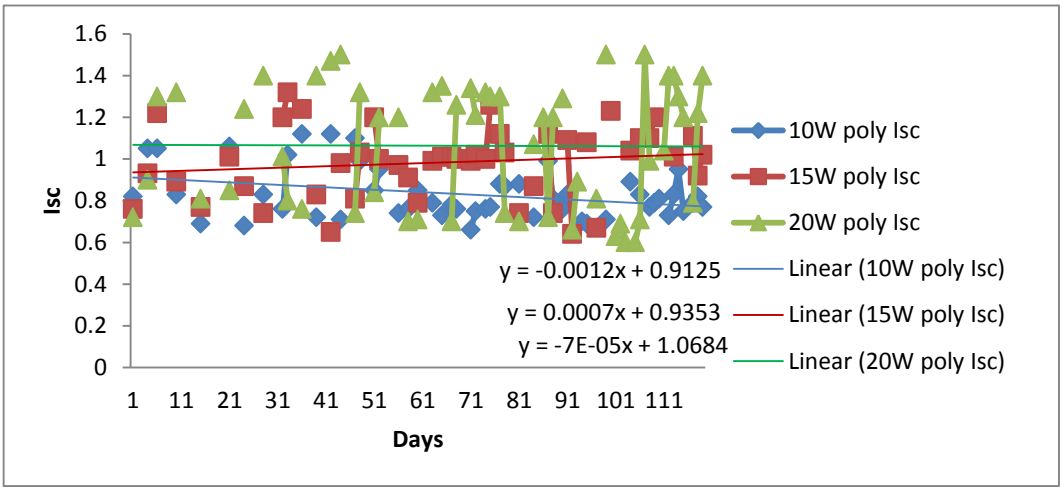

Figure 5.8: Graph of I_{sc} against number of days for the polycrystalline modules

Figure 5.9 is a graph of I_{sc} against number of days for the amorphous modules. From the graphs it is noted that there is very little variation in the amount of current produced by the three modules. Thus the I_{sc} of the modules is found not to degrade with the time of exposure.

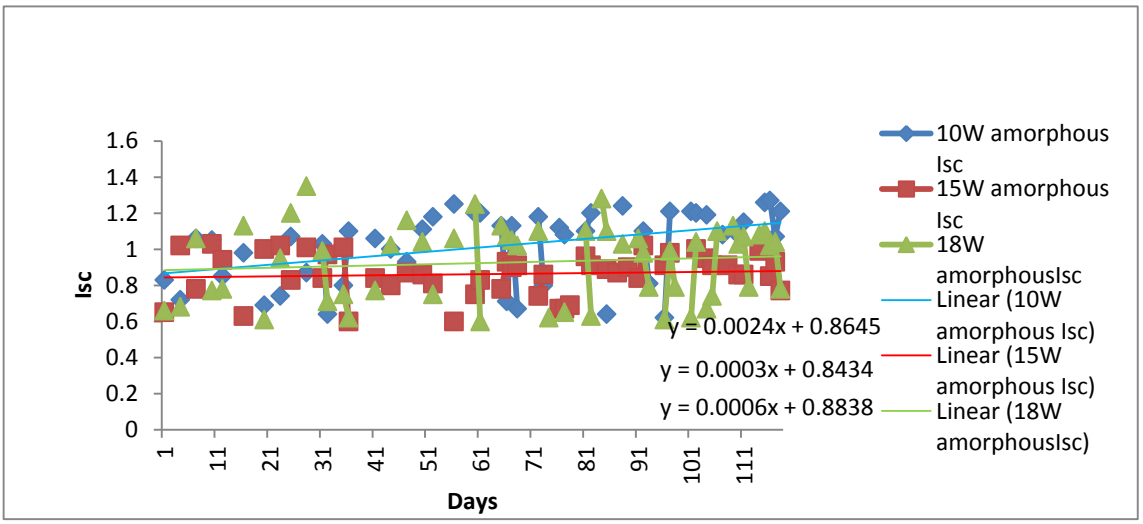

Figure 5.9: Graph of I_{sc} against number of days for the amorphous modules

5.2.3 Measured Maximum Power (P_{max})

The measured P_{max} was found to be below the P_{max} specified by the manufacturers in most of the modules other than the 10W mono crystalline which was giving 10.7W and 10W polycrystalline with 11.4W. The 10W polycrystalline module indicated a higher rate of degradation as compared to the 15W and 20W polycrystalline modules. The daily inspection of the modules revealed cells that are damaged as a result of overheating as seen in figure 5.13.

Figure 5.10 is a graph of maximum power against the number of days for the mono crystalline modules. From the graphs, the 10W mono crystalline modules registered a higher rate of degradation while the 20W mono crystalline had the least.

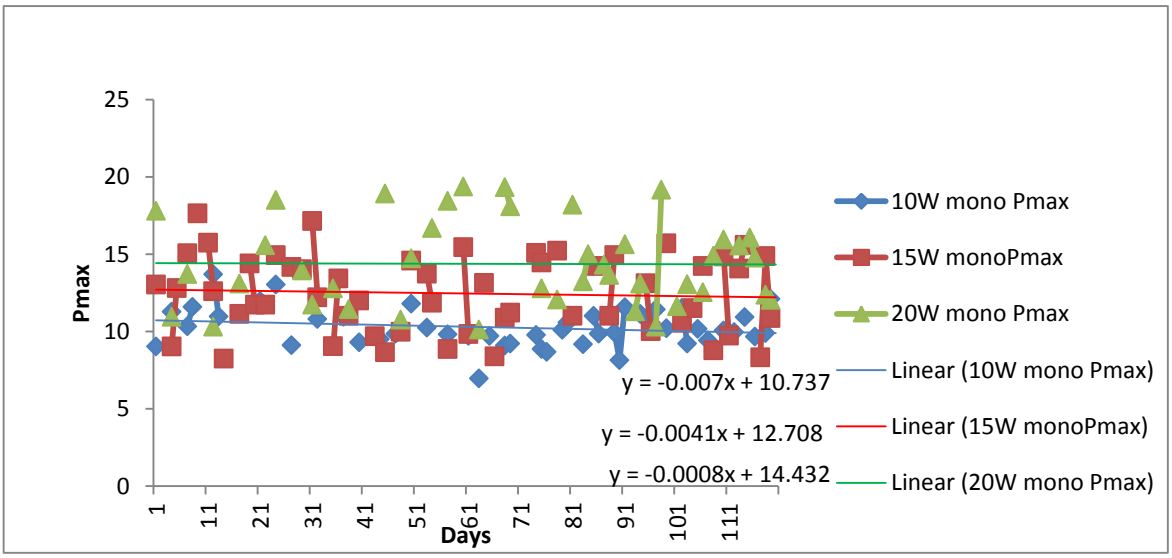

Figure 5.10: Graph of maximum power (P_{max}) against number of days for the mono crystalline

Figure 5.11 is a graph of maximum power (P_{max}) against the number of days for the polycrystalline modules. From the graphs the 10W polycrystalline module degraded more while the 15W module had the least rate of degradation.

Figure 5.12 is a graph of maximum power (P_{max}) against number of days for the amorphous module type. From the graph it is noted that the 15W amorphous module had a higher rate of degradation compared with the other amorphous modules. It is also noted that the maximum power quoted by manufacturers did not match the measured power of day one in the three modules.

Figure 5.13 is a picture of a 10W polycrystalline module. It shows a portion of cells that were damaged as a result of overheating on the module. This caused the 10W polycrystalline module to register a higher rate of degradation in comparison with the others.

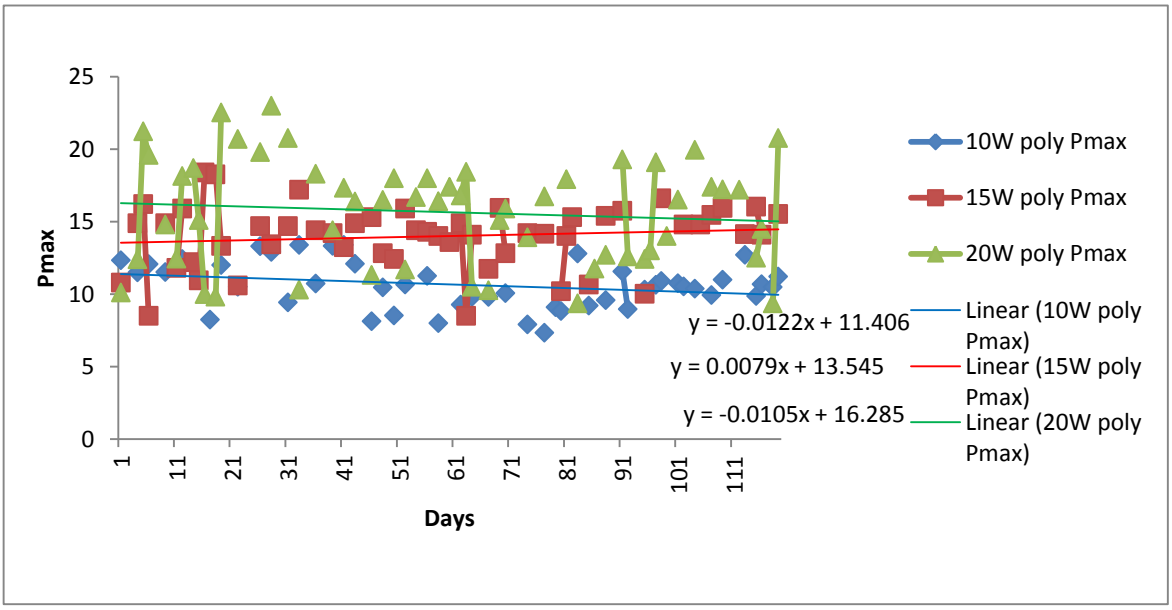

Figure 5.11: Graph of maximum power (P_{max}) against number of days for the polycrystalline modules

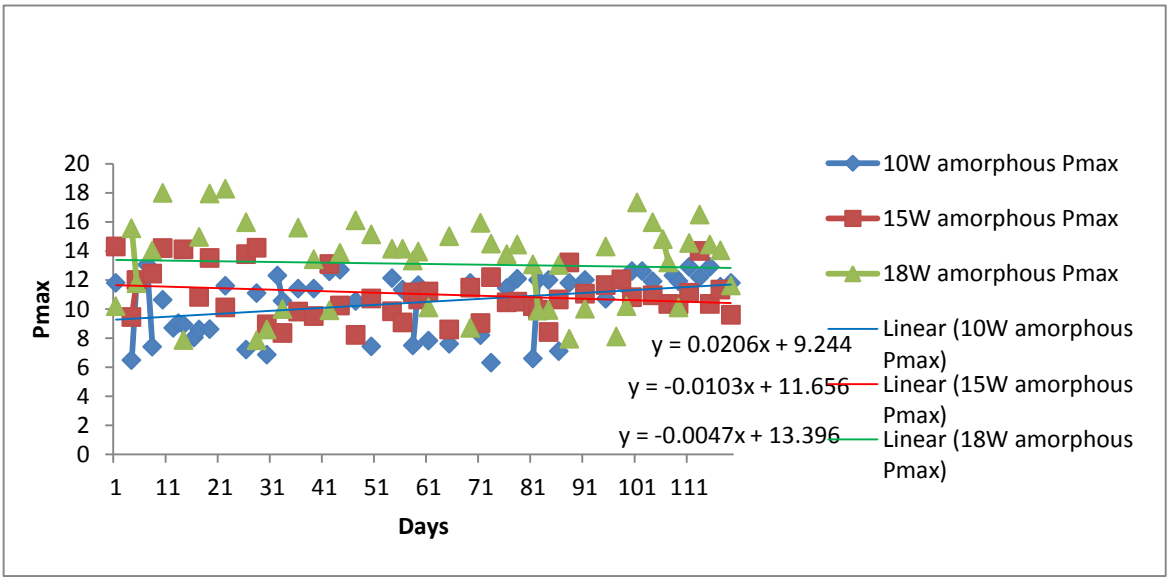

Figure 5.12: Graph of maximum power (P_{max}) against number of days for the amorphous modules

Figure 5.13: Picture of the 10W polycrystalline module defect

5.2.4 Measured Efficiency

The efficiency of the modules was found to have degraded within the first four months of exposure. The 20W mono crystalline module had the lowest efficiency compared with the other mono crystalline modules. This was attributed to defects which may have gone unnoticed during the time of manufacture. The 10W polycrystalline module had the highest rate of degradation compared with the other polycrystalline modules. The amorphous module type had the lowest efficiency of less than 6 % among the three technologies that were studied.

Figure 5.14 is a graph of efficiency against number of days for the mono crystalline modules. It is noted that the 10W mono crystalline module had a higher rate of degradation compared with the other three modules. The 20W module had the least efficiency while the 15W module had the highest.

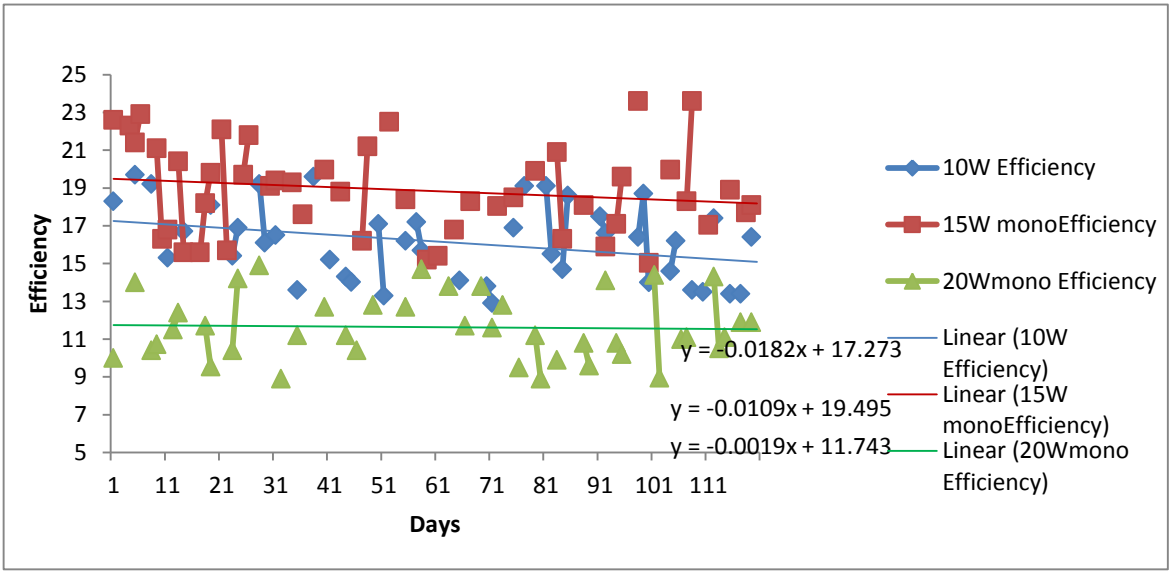

Figure 5.14: Graph of efficiency against number of days for the mono crystalline modules

Figure 5.15 shows a graph of variation of efficiency with number of days of exposure for the polycrystalline modules. From the graph, rapid drop in efficiency is observed. The 10W polycrystalline module has been found to degrade faster as compared to the 15W and 20W modules.

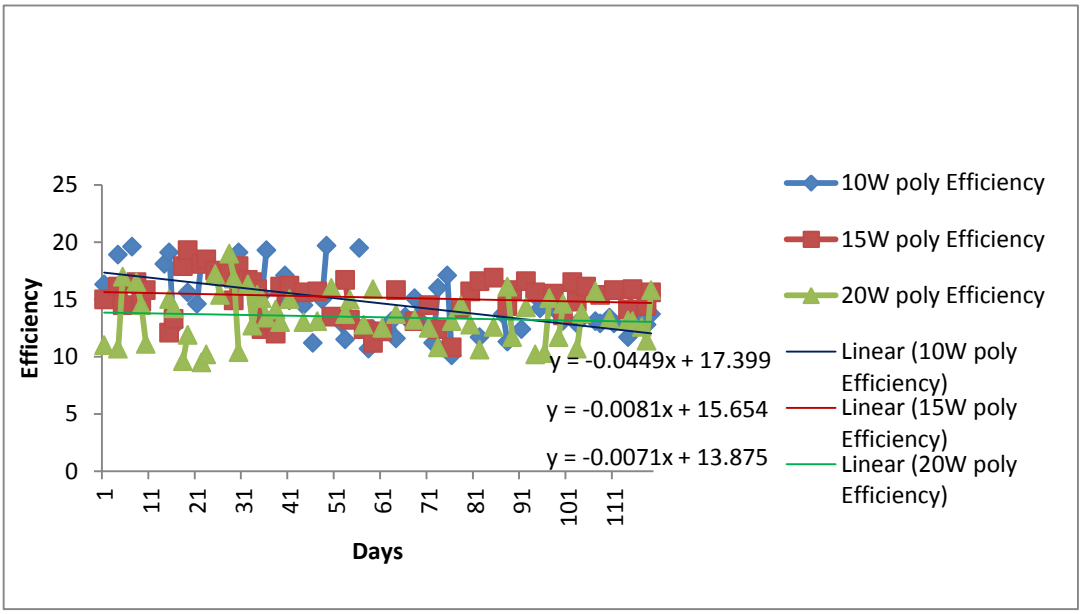

Figure 5.15: Graph of efficiency against number of days for the polycrystalline modules

Figure 5.16 shows a graph of variation of efficiency of amorphous modules with the number of days of exposure. From the graph it is observed that there is a drop in efficiency in the three modules with the 15W module degrading faster than the others.

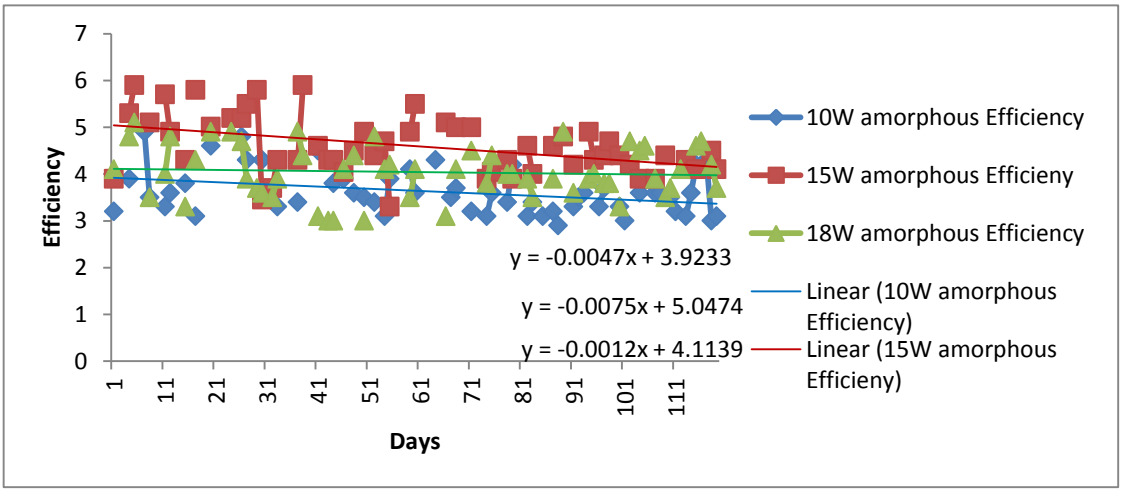

Figure 5.16: Graph of efficiency against number of days for the amorphous modules

5.3 Summary

1. The modules indicate a decrease in V_{oc} with time. The V_{oc} of amorphous modules indicates a higher rate of degradation compared to the mono crystalline and polycrystalline modules. Within the first thirty days of exposure, the amorphous modules clearly show the Staebler -Wronki degradation effect.

2. The short circuit current (I_{sc}) of the three technologies indicate a very small change with the number of days of exposure. This is not unusual since I_{sc} unlike the V_{oc} indicates a very minimal change with time of exposure.

3. The maximum power (P_{max}) of all the modules indicates a degradation trend. It was also noted that the P_{max} quoted by manufactures in most of the modules could not match the measured P_{max} for day 1.

4. The daily inspection on the modules revealed a defect in the 10W polycrystalline module that highly contributed to its low performance.

5. The efficiency of the amorphous modules was found to range between 3% - 5%which was low compared that of mono crystalline and polycrystalline modules whose efficiency was above 10%.

CHAPTER SIX

CONCLUSIONS AND RECOMMENDATIONS

6.1 Conclusions

The research investigated the performance of silicon-based photovoltaic modules that are found in the Kenyan market. The main contribution of this work is to equip the photovoltaic module consumers within the Kenyan market with the knowledge on the modules available in the market, and their performance when exposed to the tropical climate. It was clear that all the modules experienced degradation. While all the modules degraded, the efficiencies of the mono crystalline and polycrystalline module type was quite high (above10%) while the efficiency of the amorphous modules was quite low (5% and below). It was also noted that at high irradiance (above 800W/m^2) the temperatures of the mono crystalline modules and polycrystalline modules were higher compared to the amorphous module. The maximum power of the modules was found to be lower than that quoted by the manufactures in most cases.

6.2 Recommendations

This study has made some meaningful contribution by evaluating the performance of photovoltaic modules available in the Kenyan market. However, there still some considerations that could be made to equip the Kenyan photovoltaic module consumers with the knowledge of the modules that can serve them best and give them the value for their money. For this reason further work need to be done on the following areas to equip the user adequately: Determining the performance parameters of the modules when driving a load. It is expected that the photo degradation experienced by the modules differs depending on whether the module is under load, at short circuit conditions or at open circuit condition.

The performance parameters of the modules should be determined for a whole year so that the full weather patterns can be taken into account in establishing the stability of the modules.

Since there are other module technologies and new manufacturers have joined the photovoltaic market, it is important to compare their performance with those that are existing so that the module consumers in Kenya can get those that can serve them best.

There is also a need for the government of Kenya policy makers to set up a well-equipped laboratory for testing the modules that are imported from time to time to shield the Kenyan consumer from unhealthy exploitation as well as making sure that the country does not become a damping site for inferior modules.

Finally, it is important that the performance of the modules be evaluated while using a solar tracking device so that maximum irradiance is utilized.

REFERENCES

Abdul J., Nazar A. and Omega A. (2012). Simulation on Maximum Power Point Tracking of the Photovoltaic Module using LabVIEW. *International journal of Advanced Research in Electrical, Electronics and Instrumentation Engineering,* **1**: 1-10.

Agroui K., Hadj A., Pellegrino M., Giovanni F. and Mahammad I. (2011). Indoor and Outdoor Photovoltaic Modules Performances Based on Thin Films Solar Cells. *Research and Applications. Renewable Energy,* **14**: 469-480.

Azhar G. and Abdul M. (2012). The performance of Three Different Solar Panels for Solar Electricity Applying Solar Tracking Device Under The Malysian Climate Condition. *Energy and Environment Research,* **2** : 235-243.

Akachuku B. (2003). Prediction of optimum Angle of Inclination for flat plane solar collector in Zaria, Nigeria. *Agricultural Engineering International Journal, Commision Internationale du Genie Rural,* **13**:1-11.

Carr A. (2005). A Detailed Performance Comparison of PV Modules of Different Technologies and the Implications for the PV System design Methods. *Phd Thesis*; Murdock University. Western Australia.

Chris D. (2011). Guide in interpreting I-V curves measurement of PV arrays. *Application note PV* -600-1. *http://www.Solmetric.com (2011)* accessed on 17.01.2013.

Cornaro C. and Musella D. (2010). Performance Analysis of PV Modules of Various Technologies After More than One Year of Outdoor Exposure in Rome, Italy.

Danny H. and Tonny N. (2007). Determining the Optimum Angle of Tilt and Orientation for Solar Energy Collection Based on Measured Solar radiance Data. *International Journal of Photo energy,* 12: 1-10.

Duke R., Graham S., Mark H., Arne J., Daniel M., Osawa B., Simone P. and Erika W. (1999). Field Performance Evaluation of Amorphous Silicon (a-Si) Photovoltaic Systems in Kenya: Methods and measurements in Support of a Sustainable Commercial Solar Energy Industry. *A Project of Energy Alternatives Africa (EAA) and Renewable Appropriate Energy Laboratory (RAEL) and Energy and Resources Group (ERG),* University of California, Berkeley.

Dunlop E. and Halton D. (2006). The Performance of Crystalline Silicon Photovoltaic Solar Modules after 22 years of Exposure**.** *Progress in Photovoltaic. Research applications,* **7**:16-23.

Ethan W. and Hsinjin E. (2012). Failure Modes Evaluation of PV Materials Degradation Approach. *PV Asia Pacific Conference. Energy Procedia,* **33**: 256-264.

George M., Bastian Z., Matthew N. and George E. (2010). Perfomance of PhotoVoltaics Under Actual Operating Conditions. *In Tech.Third Generation PhotoVoltaics,* **3: 245-263.**

Higa M. and Lord S. (2002). An introduction to LabVIEW exercise for Electronic Class. 32nd *Annual frontiers in Education,* **1**: 6.

http://www.Kenya-Information-Guide.com/Kenya-Weather.html.Accessed on 07.05.2013.

Ibrahim D. (1995). Optimum Tilt Angle for Solar Collectors used in Cyprus. *In the Proceedings of Renewable Energy,* **6**: 813-819.

Jeffrey K. and Jim T. (2006). LabVIEW for Everyone. *3rd edition prentice hall.* Indiana, U.S.A, 56-134.

Kacira M., Simsek M., Barbur Y. and Demirkol S. (2004). Determining Optimum Tilt Angles of Photovoltaic Panels in Sanliurfa, Turkey. *Renewable Energy,* **29**: 1265-1275.

Malik A., Ming L., Sheng T. and Blundell M. (2010). Influence of Temperature on the Performance of Photovoltaic Polly crystalline Silicon Module in the Bruneian Climate. *A SEAN Journal for Science and Technology Development,* **26**: 61-72.

Manuel V. and Ignacio R. (2008). Photovoltaic Module Relaibility Model Based on Field Degradation Studies. *Progrees Report on Photovoltaics: Research and Applications,* **10**: 825-1002.

Pavlovic T., Pavloc J. Pantic L. and Kostic L. (2010). Determining the Optimum Tilt Angles and Orientation of Photovoltaic Panels in Nis`,Serbia. *Anurs. Cmat*.1002, **10**: 151-156.

Osterwald C., Anderberg A., Rummel S. and Ottoson L. (2002). Degradation Analysis of Weatherd Crystalline-Silicon PV Modules. *National Renewable Energy Laboratory,* **10**: 96-108.

Prashanthani S., Adibah M. Balbir S. and Norani M. (2011). Optimum Tilt Angle and Orientaion of Stand-Alone Photovoltaic Electricity Generation Systems for Rural Electrification. *Journal of Applied Sciences,* **11**:1219-1224.

Rakovect J. and Klemen Z. (2011). Orientation and Tilt Dependence of a Fixed PV Array Energy Yield Based on Measurements of Solar Energy and Ground Albedo- A Case Study of Slovenia. *Progress Report on Photovoltaics: Research and Applications*, **13**: 42-51.

René J. (2005). *Introduction to polymer solar cells*. Eindhoven University of Technology, Netherlands. 3Y280.

Renewable Energy in developing Countries -Wikipedia. Org. accessed on 4.05.2014.

Rong P., Joseph K., Govindasamy T. (2011). Degradation analysis of Solar Photovoltaic Modules: Influence of Environment Factor. *In the proceedings of Reliability and Maintainability Symposium,* **15**: 24-27.

Ryan M., Dirk C. and Sarah R. (2012). Outdoor PV Module Degradation of Current-Voltage Parameters. *National Renewable Energy Laboratory 1617 Cole Boulevard. Golden, Co 80401.*

Siddiqui R., Kumar R., Jha G. and Bajpai U. (2014). Performance Analysis of Polycrystalline Silicon PV Modules on the Basis of Indoor and Outdoor Conditions. *International Journal of Current Engineering and Technology,* **14**: 35-47.

APPENDICES

APPENDIX A

Table A.1: Manufacturers Specifications for Mono Crystalline Modules

Module type	manufacturer	I_{sc} (A)	V_{oc} (V)	I_{mp} (A)	V_{mp} (V)	Efficiency (%)	Fill Factor (FF)
10W mono crystalline	Sunshine solar- Germany	0.63	22.05	0.57	17.5	14	0.72
15W mono crystalline	Euro solar	0.95	21.8	0.87	17.2	18.3	0.72
20W mono crystalline	Euro solar	1.28	21.8	1.16	17.2	13.5	0.72

Table A.2: Manufacturers Specifications for Polycrystalline Modules

Module type	Manufacturer	I_{sc} (A)	V_{oc} (V)	I_{mp} (A)	V_{mp} (V)	Efficiency (%)	Fill Factor (FF)
10W	Robin:Shangai:Talen power Ltd,China	0.65	21.6	0.57	17.5	12	0.71
15W	Shunshine: Germany	0.95	22.05	0.85	17.5	15	0.71
20W	Shunshine: Germany	1.27	22.05	1.14	17.5	15.3	0.71

Table A.3: Manufacturers Specifications for Amorphous Modules

Module type	manufacturer	I_{sc} (A)	V_{oc} (V)	I_{mp} (A)	V_{mp} (V)	Efficiency (%)	Fill Factor (FF)
10W	Trony Solar Corporation	0.85	26.7	0.56	18	2.7	0.44
15W	France	1.0	25	0.75	16	4.5	0.48
18W	Phoenix	1.0	21.0	0.87	19	4.4	0.79